Combinatorial and Continuous Models for the Optimization of Traffic Flows on Networks

A. Fügenschuh, M. Herty, A. Klar, A. Martin

March 1, 2004

Abstract

A hierachy of simplified models for traffic flow on networks is derived from continuous traffic flow models based on partial differential equations. The hierachy contains nonlinear and linear combinatorial models with and without dynamics. Optimization problems are treated for all models and numerical results and algorithms are compared.

1 Introduction

Modelling and simulation of traffic flow on highways has been investigated intensively during the last years. On the one hand models describing detailed traffic dynamics on single roads have been constantly developed and improved, see [32, 31, 27, 14, 30, 1, 23, 13, 11, 8, 12] and many others. To describe traffic flow on networks such detailed dynamic models based on partial differential equations have been used in [18, 7]. However, the number of roads which can be treated with such an approach is restricted, in particular, if optimization problems have to be solved. On the other hand large traffic networks with strongly simplified dynamics or even static description of the flow have been widely investigated [6, 10, 21, 24, 28]. In particular, optimal control problems for traffic flow on networks arising from traffic management, see for example [26, 3], are a major focus of research in this field.

The purpose of the present investigation is to derive and develop a hierachy of simplified dynamical models based on the 'correct' dynamics described by partial differential equations. These models should include reasonable dynamics and, at the same time, they should be solvable for large scale networks. Special focus is on optimal control problems and optimization techniques. We start with macroscopic models based on partial differential equations. Two such models were introduced by Holden/Risebro [18], resp. Coclite/Piccoli [7]. In particular, dealing with optimal control questions for such large scale networks where the flow is described by partial differential equations is very expensive from a computational point of view, see for [16, 17]. Therefore, we concentrate in the present paper on the derivation of simplified dynamic models derived

from the models based on partial differential equations. The resulting models are network models which are based on nonlinear algebraic equations or combinatorial models based on linear equations. In the simplest case well known static combinatorial models like min-cost flow models are obtained. For the different models we study optimal control problems and various optimization methods, i.e., combinatorial and continuous optimization techniques. Using strongly simplified models large scale networks can be optimized with combinatorial approaches in real-time. However, including more complex dynamics reduces the advantage of the combinatorial algorithms compared to continuous optimization procedures.

We note that for the linear models there is a strong connection to the traffic flow models proposed by Möhring et al. see, for example [24]. Especially the occurence of the so-called transit-times shows the close relation between the models. However, the cost functional for the linear problem differs due to the derivation starting with partial differential equations. For more details see Remark 4.3.

2 Continuous traffic flow models

The starting point is a macroscopic traffic flow model on networks. We give a brief review of the model. Further details and more general situations are treated in [7, 16]. We consider a network of roads as follows:

Definition 2.1. *A traffic flow network is a finite, connected directed graph. For some traffic road map we introduce a graph $G = (V, E)$ where the edges correspond to the roads and the vertices to the junctions. With each edge j, $j = 1, \ldots, |E|$ we associate an intervall $[a_j, b_j]$ representing the location x at the corresponding road, with the interpretation $x = a_j$ if we are at the head of edge j and $x = b_j$ if we are at the tail of edge j. The vertices of the graph are labelled by $v = 1, \ldots, |V|$. At a single junction v the set of indices of ingoing roads is denoted by δ_v^- and the set of outgoing roads by δ_v^+.*

On each edge j, the traffic dynamics are described by a model based on partial differential equations for the density $\rho_j(x,t), x \in [a_j, b_j], t \geq 0$. We use the well-known Lighthill-Whitham equations [29] to model the evolution of the density. Hence the following equations are assumed to hold on the network away from junctions:

$$\partial_t \rho_j(x,t) + \partial_x f_j(\rho_j(x,t)) = 0, \qquad \forall j = 1, \ldots, |E|,\ x \in [a_j, b_j], t \geq 0 \quad (2.1)$$

$$\rho_j(x,0) = \bar{\rho}_j(x) \qquad \forall x \in [a_j, b_j], \quad (2.2)$$

where $f_j(\rho) = \rho u_j^e(\rho)$ and $u_j^e(\rho)$ is the fundamental diagram and $\bar{\rho}_j(x)$ are given initial values.

A solution ρ_j $j = 1, \ldots, |E|$ to the network problem should satisfy flux

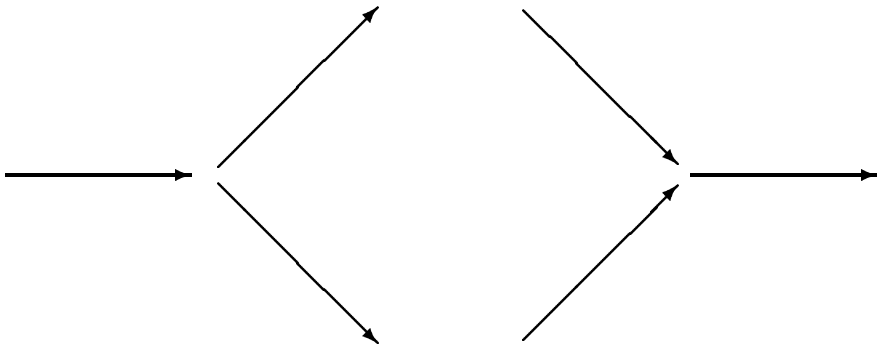

Figure 1: Considered types for a junction v. The used notation is $\delta_v^- = \{j_1, j_2\}$, $\delta_v^+ = \{j_3\}$ (left), resp. $\delta_v^- = \{j_0\}$, $\delta_v^+ = \{j_1, j_2\}$ (right part of the figure).

conservation through junctions, i. e., for all $v = 1, \ldots, |V|$ we have

$$\sum_{j \in \delta_v^-} f_j(\rho_j(b_j, t)) = \sum_{j \in \delta_v^+} f_j(\rho_j(a_j, t)) \quad \forall t \in (0, \infty). \tag{2.3}$$

To obtain a well-defined problem we have to impose further boundary conditions in the sense of [2]. Those conditions describe the coupling of different roads at a junction and satisfy (2.3). An overview of possible models for junctions and the corresponding boundary values for the equations (2.1) can be found in [16]. For the following derivations we restrict ourselves to the Coclite/Piccoli model of junctions [7]. For non-constant initial data $\bar{\rho}_j(x)$ the obtained boundary conditions can not be given explicitly. They are well-defined in the case of constant initial data and obtained as the limit of an approximation, see [7, 9, 19]. However, in certain cases and under some restrictions one can derive explicit formulas for the boundary values. We briefly describe the Coclite/Piccoli coupling conditions for special geometries.

We restrict ourselves for simplicity to networks with only two types of junctions with a total of three incident roads, see Figure 1. We assume that f_j is defined on $[0, \rho_{j,\max}]$ and assume that f_j is smooth, concave with single maximum. Define

$$M_j = \max f_j(\rho), \ \sigma_j = \operatorname{argmax} f_j(\rho). \tag{2.4}$$

We consider the case of a single junction v and constant initial data $\bar{\rho}_j$. Coclite/Piccoli introduced additional conditions for a junction by considering Riemann problems on the in- and outgoing roads. To be more precise, assume we have given values $\tilde{p}_j \in \mathbb{R}^+$ and the initial value $\bar{\rho}_j \in \mathbb{R}^+$. We consider the

following problem:

$$\begin{aligned}
&\partial_t \rho_j + \partial_x f_j(\rho_j) = 0 \\
&j \in \delta_v^+ : \rho_j(x,0) = \begin{bmatrix} \bar{\rho}_j & x > a_j \\ \tilde{p}_j & x \le a_j \end{bmatrix} \text{ resp.} \\
&j \in \delta_v^- : \rho_j(x,0) = \begin{bmatrix} \tilde{p}_j & x \ge b_j \\ \bar{\rho}_j & x \le b_j \end{bmatrix}
\end{aligned} \tag{2.5}$$

A solution ρ_j of (2.5) satisfies also (2.1). We have a degree of freedom in choosing the values $\tilde{p}_j$. Since the conservation of flux (2.3) holds, there are certain restriction on $\tilde{p}_j$. They can be given explicitly by (2.7) using the following definition of τ:

$$\forall \rho \exists \tau = \tau_j(\rho) : \tau \neq \rho, f_j(\tau) = f_j(\rho). \tag{2.6}$$

The restrictions are

$$\begin{aligned}
&j \in \delta_v^- : \\
&\tilde{p}_j \in \begin{bmatrix} \{\bar{\rho}_j\} \cup]\tau_j(\bar{\rho}_j), \rho_{j,\max}] & \text{if } \bar{\rho}_j < \sigma_j \\ [\sigma, \rho_{j,\max}] & \text{if } \bar{\rho}_j \ge \sigma_j \end{bmatrix} \\
&j \in \delta_v^+ : \\
&\tilde{p}_j \in \begin{bmatrix} [0, \sigma_j) & \text{if } \bar{\rho}_j < \sigma_j \\ \{\bar{\rho}_j\} \cup [0, \tau_j(\bar{\rho}_j)[& \text{if } \bar{\rho}_j \ge \sigma_j \end{bmatrix}.
\end{aligned} \tag{2.7}$$

Depending to which intervall $\tilde{p}_j$ belongs, the wave generated by the Riemann problem (2.5) is either a shock wave or a rarefaction wave. But still, there are many possible choices for $\tilde{p}_j$ depending on the values of $\bar{\rho}_j$. Therefore Coclite/Piccoli introduced more constraints.

Case 1: Consider a single junction v where road j_0 disperse in two roads j_1 and j_2. A value $\alpha_v \in \mathbb{R}$ with $0 < \alpha_v < 1$ specifying the percentage of drivers coming from road j_0 and driving to j_1 is introduced. (2.3) reads

$$\begin{aligned}
&f_{j_1}(\rho_{j_1}(a_{j_1}+,\cdot)) = \alpha_v f_{j_0}(\rho_{j_0}(b_{j_0}-,\cdot)) \\
&f_{j_2}(\rho_{j_2}(a_{j_2}+,\cdot)) = (1-\alpha_v) f_{j_0}(\rho_{j_0}(b_{j_0}-,\cdot)).
\end{aligned} \tag{2.8}$$

Unique values $\tilde{p}_j, j = j_0, j_1, j_2$, can be found by solving the maximization problem

$$\max f_{j_0}(\tilde{p}_j) \text{ s.t. } (2.7), (2.8), (2.5) \tag{2.9}$$

Equation (2.9) does not allow an explicit representation of the boundary conditions. If we neglect the possibility of shock waves, especially backwards going shock wave on the incoming street j_0, the situation is much simpler. Therefore we assume in the following

$$\bar{\rho}_j, \rho_j(x,t) \le \sigma_j, \ \forall j. \tag{2.10}$$

Since we omit shock waves on j_0 we obtain instead of the maximization problem (2.9) an explicit formula for calculating $\tilde{p}_j$:

$$\begin{aligned} &\tilde{p}_j = \bar{\rho}_j \; j = j_0 \\ &f_{j_1}(\tilde{p}_{j_1}) = \alpha_v f_{j_0}(\tilde{p}_{j_0}) \\ &f_{j_2}(\tilde{p}_{j_2}) = (1-\alpha_v) f_{j_0}(\tilde{p}_{j_0}). \end{aligned} \tag{2.11}$$

Equation (2.11) is well-defined due to (2.10) and yields unique values $\tilde{p}_{j_1}, \tilde{p}_{j_2}$.

Remark 2.1. *Coclite/Piccoli proved the existence and uniqueness of admissible solutions satisfying (2.9) for a single junction with constant initial data. They generalized this result to prove existence for networks where for each junction v we have $|\delta_v^-| + |\delta_v^+| \leq 4$ and the initial data $\bar{\rho}_j$ has bounded total variation. For more details we refer to [7].*

Case 2: Consider a single junction v where roads j_1 and j_2 merge to j_3. Flux conservation through the junction implies

$$f_{j_3}(\rho_{j_3}(a_{j_3}+,\cdot)) = f_{j_1}(\rho_{j_1}(b_{j_1}-,\cdot)) + f_{j_2}(\rho_{j_2}(b_{j_2}-,\cdot)). \tag{2.12}$$

In the same spirit as above we define unique values $\tilde{p}_j, j = j_i, i = 1,2,3$ by a procedure suggested in [16]: Define maximal possible fluxes by

$$\begin{aligned} &j \in \delta_v^- = \{j_1, j_2\} : \\ &\gamma_j = \begin{bmatrix} f_j(\bar{\rho}_j) & \text{if } \bar{\rho}_j < \sigma_j \\ M_j & \text{if } \bar{\rho}_j \geq \sigma_j \end{bmatrix} \\ \\ &j \in \delta_v^+ = \{j_3\} : \\ &\gamma_j = \begin{bmatrix} M_j & \text{if } \bar{\rho}_j < \sigma_j \\ f_j(\bar{\rho}_j) & \text{if } \bar{\rho}_j \geq \sigma_j \end{bmatrix} \end{aligned}$$

and solve the maximization problem:

$$\begin{aligned} &\text{If } \gamma_{j_1} + \gamma_{j_2} > \gamma_{j_3} \max \sum_{j \in \delta_v^-} f_j(\tilde{p}_j) \text{ s.t. } (2.12), (2.7) \text{ and } f_{j_1}(\tilde{p}_{j_1}) = f_{j_2}(\tilde{p}_{j_2}) \\ &\text{If } \gamma_{j_1} + \gamma_{j_2} \leq \gamma_{j_3} \max \sum_{j \in \delta_v^-} f_j(\tilde{p}_j) \text{ s.t. } (2.12), (2.7). \end{aligned} \tag{2.13}$$

Again we obtain an explicit representation of the boundary conditions when assuming (2.10).

$$\begin{aligned} &\tilde{p}_j = \bar{\rho}_j \; j = j_1 \text{ and } j = j_2 \\ &f_{j_3}(\tilde{p}_{j_3}) = \sum_{j \in \delta_v^-} f_j(\tilde{p}_j) \end{aligned} \tag{2.14}$$

Now, optimal control problems can be investigated. Typically, the time spent by the drivers in the network is minimized. This means we consider the functional

$$J(\alpha_1, \ldots, \alpha_{|V|}) = \int_0^T \sum_{j=1}^{|E|} \int_{a_j}^{b_j} \rho_j(x,t) dx dt. \tag{2.15}$$

This functional has to be minimized with respect to the control variables α_v. We solve the problem:

$$\min_{0<\alpha_1,\cdots,\alpha_{|V|}<1} J(\alpha_1,\ldots,\alpha_{|V|}) \tag{2.16}$$

subject to: ρ_j is solution of (2.1) with coupling conditions
at the junctions given by (2.9) and (2.13).

A solution to this problem yields an optimal distribution of a traffic flow in a network including all dynamics, like jam propagation etc.

Alternatively we can optimize the above functional in the case of no backwards going shock wave. This implies replacing conditions (2.9) and (2.13) by (2.11) and (2.14). However, even in this case optimization of networks with a large number of roads in reasonable time is beyond any computational possibility.

3 Simplified Nonlinear Model

In this section the traffic flow model based on partial differential equations is reduced to a system of algebraic equations, c.f. [17]. This is achieved by considering a simplified situation concerning the inflow into the network and tracking single waves running through the network. In contrast to the static network models often used by traffic engineers the present approach still contains simplified dynamics, being at the same time not much more complicated and expensive from a computational point of view. For the following we assume that no backwards going shock waves appear, this means that the traffic is optimized in such a way that no traffic jam occurs. We start with an initially empty network and refer to the end of the section for the case of partially filled networks. Moreover, we restrict for the moment to constant inflow $\rho_{j,0}$ applied as boundary condition at the incoming road to the network. For the geometry of the network we use the same assumptions as in the previous section, i. e., we assume to have only junctions connecting at most three roads, labelled like in Figure 1.

We assume to have an initially empty network, i. e.,

$$\rho_{j,0}(x) = 0.$$

The assumption of no backwards going shock waves is imposed as in (2.10), i. e.,

$$\rho_j(x,t) \leq \sigma_j \ \forall j.$$

We assign two values $p_j \in \mathbb{R}$ and $t_j \in \mathbb{R}^+$ to each road j of the network. The value p_j is an approximation of the density $\rho_j(x,t)$ while t_j denotes the arrival time of a wave at road j. The following bounds are obvious.

$$0 \leq p_j \leq \sigma_j, \ 0 \leq t_j \leq T. \tag{3.1}$$

Due to (2.10) we can express the coupling conditions (2.11) and (2.14) in the form (2.11). We translate them in terms of p_j and obtain:

Case 1:

$$\begin{aligned}\delta_v^- &= \{j_0\}, \delta_v^+ = \{j_1, j_2\}\\ p_{j_1} &= f_{j_1}^{-1}(\alpha_v f_{j_0}(p_{j_0}))\\ p_{j_2} &= f_{j_2}^{-1}((1-\alpha_v) f_{j_0}(p_{j_0})).\end{aligned}$$

Case 2:

$$\begin{aligned}\delta_v^- &= \{j_1, j_2\}, \delta_v^+ = \{j_3\}\\ p_{j_3} &= f_{j_3}^{-1}(f_{j_1}(p_{j_1}) + f_{j_2}^{-1}(f_j(p_{j_2})))\end{aligned}$$

For the ingoing roads to the network we set $p_j = \rho_{j,0}$. In Case 1 the parameters $0 < \alpha_v < 1$ distributes traffic at junction v in the direction of road i. Hence, p_j is determined solely by fulfilling the coupling conditions at the junctions.

Remark 3.1. *As an example note that for a flux function of the type* $f_j(x) = 4x(1 - x/M_j)$ *the conditions read* $2p_{j_1} = M_{j_1} - \sqrt{M_{j_1}^2 - \alpha_v M_{j_1} f_{j_0}(p_{j_0})}$ *and similar for* p_{j_2}. *For the other junction we obtain* $2p_{j_3} = M_{j_3} - \sqrt{M_{j_3}^2 - M_{j_3}\chi}$ *with* $\chi = f_{j_1}(p_{j_1}) + f_{j_2}(p_{j_2})$.

We model the dynamics in the following way: the times t_j describe an approximation of the arrival times of the waves (generated as solutions to the hyperbolic equation (2.1)) at $x = a_j$ of road j. Since we cannot track the whole wave we use as an approximation a discontinuity. Then the times t_j defined by (3.2) and (3.3). In more detail, we have initially a Riemann problem

$$\partial_t \rho_j + \partial_x f_j(\rho_j) = 0, \quad \rho_j(x,0) = \begin{bmatrix} p_j & x \le a_j \\ 0 & x > a_j \end{bmatrix}$$

with concave fluxfunction f_j. A rarefaction wave is the correct solution of the above problem. We simplify this by approximating the wave by a discontinuity. We restrict ourselves to track only one wave on each road. The speed of the wave is approximated with the so-called "Rankine-Hugoniot speed"

$$s_j = \frac{f_j(p_j)}{p_j}.$$

The arrival times of the rarefaction wave are approximated as follows: For the ingoing road j_0 we set $t_{j_0} = 0$. In the case of a junction, where one road j_0 disperse in two others j_1, j_2 we set

$$t_{j_1} = t_{j_2} = t_{j_0} + \frac{b-a}{s_{j_0}}. \tag{3.2}$$

In the case of a junction with two incoming roads j_1, j_2 and one outgoing road j_3 the situation is more complicated. We set

$$t_{j_3} = (t_{j_1} + \frac{b-a}{s_{j_1}})\frac{p_{j_1}}{p_{j_1}+p_{j_2}} + (t_{j_2} + \frac{b-a}{s_{j_2}})\frac{p_{j_2}}{p_{j_1}+p_{j_2}}. \tag{3.3}$$

This choice is motivated by the following calculations: Let $t^{(1)} < t^{(2)}$ denote the time, when the dicontinuity from road j_1 and j_2 reach the beginning of road j_3 with the values p_{j_1} and p_{j_2}. We again assume to have one shock on road j_3 instead of rarefaction waves. The travelling speeds are given by $s^{(1)} = \frac{f_{j_3}(p_{j_1})}{p_{j_1}}$ and $s^{(2)} = \frac{f_{j_3}(p_{j_3}) - f_{j_3}(p_{j_1})}{p_{j_3} - p_{j_1}}$. The values p_{j_3} are determined by the coupling condition, i.e. $f(p_{j_3}) = f(p_{j_1}) + f(p_{j_2})$. Then we have

$$\begin{aligned}\int_0^T \int_a^b \rho_{j_3}(x,t)dxdt &= (T - t^{(1)})(b-a)p_{j_1} - \frac{p_{j_1}}{2s^{(1)}}(b-a)^2 \\ &+ (T - t^{(2)})(b-a)(p_{j_3} - p_{j_1}) - \frac{p_{j_3} - p_{j_1}}{2s^{(2)}}(b-a)^2\end{aligned}$$

The idea is to approximate the above integral by $(T - t_{j_3})(b-a)p_{j_3} - \frac{p_{j_3}}{2s_{j_3}}(b-a)^2$ with $s_{j_3} = f_{j_3}(p_{j_3})/p_{j_3}$. If f is linear, then the correct choice for t_{j_3} is

$$t_{j_3} = t^{(1)}\frac{p_{j_1}}{p_{j_1} + p_{j_2}} + t^{(2)}\frac{p_{j_2}}{p_{j_1} + p_{j_2}}. \tag{3.4}$$

This is used as approximation in the nonlinear case. Finally, to obtain formula (3.3) we use (3.4) together with $t^{(1)} = (t_{j_1} + \frac{b-a}{s_{j_1}})$ and $t^{(2)} = (t_{j_2} + \frac{b-a}{s_{j_2}})$.

Thus we have defined a purely algebraic dynamic model for traffic flow on road networks without backwards going shock waves.

It remains to reformulate the functional (2.15) in terms of the simplified nonlinear model. We assumed to have a discontinuity arrives at road j at time t_j and travels with speed s_j. Evaluating the integral $\int_0^T \int_{a_j}^{b_j} \rho_j(x,t)dxdt$ under this assumptions yields

$$\int_0^T \int_{a_j}^{b_j} \rho_j(x,t)dxdt = (T - t_j)(b_j - a_j)p_j - \frac{p_j}{2s_j}(b_j - a_j)^2.$$

Finally, the full simplified nonlinear model reads with $L_j = b_j - a_j$ and $s_j = f_j(p_j)/p_j$:

For junctions of merging type:

$$t_k = (t_i + \frac{L_i}{s_i})\frac{p_i}{p_i + p_j} + (t_j + \frac{L_j}{s_j})\frac{p_j}{p_i + p_j}$$

$$p_k = f_k^{-1}(f_i(p_i) + f_j(p_j)).$$

For junctions of dispersing type:

$$t_i = t_j = t_k + \frac{L_k}{s_k}$$

$$p_i = f_i^{-1}(\alpha_v f_k(p_k)), \quad p_j = f_j^{-1}((1 - \alpha_v)f_k(p_k)).$$

For the road entering the network:

$$p_j = \rho_0, t_j = 0.$$

The functional reads

$$J(\alpha; T, \rho_0) = \sum_{j=1}^{J}(T - t_j)L_j p_j - \frac{p_j}{2s_j}L_j^2. \tag{3.5}$$

Herein T is a fixed time and ρ_0 is the inflow to the network. It turns out that also for this simplification the minimization problem $\min J$ subject to the constraints above still needs large computation times for very large networks due to the nonlinearities in the coupling conditions for p_j and t_j. For numerical results we refer to the subsequent sections.

Remark 3.2. *The treatment of a partially filled network is also possible. Assume we have the initial densities $\bar{p}_j$ on road j given, where all values are consistent with the conditions at the junctions. $\bar{p}_j$ is constant for the whole road such that $\bar{p}_j < \sigma_j$. We start, as before, with an inflow $\rho_0 < \sigma$. Then similar considerations as the above yield the following expression for an integral on j with ($L := b - a$)*

$$\int_0^T \int_a^b \rho(x,t)dxdt = Lt_j\bar{p}_j + Lp_j(T - t_j) - \frac{p_j - \bar{p}_j}{2s_j}L^2 \tag{3.6}$$

where now s_j is given by

$$s_j = \frac{f_j(p_j) - f_j(\bar{p}_j)}{p_j - \bar{p}_j}. \tag{3.7}$$

Using this definition of s_j one can approximate the arrival times of the ingoing wave t_j in the same way as before with s_j as in (3.7).

Remark 3.3. *Nonconstant initial data, for example piecewise constant initial data, can be treated in the same way. For each wave the arrival times have to be tracked and we have to assume that the waves do not interact.*

4 Linear Models

In this section the previously introduced model is further simplified obtaining a linear model accessible to discrete optimization techniques. The basic idea is the reformulation of the above model in terms of the flux $q_j := p_j u^e(p_j)$. We introduce the notation

$$\tau_j(q_j) := \frac{1}{u^e(f_j^{-1}(q_j))} \tag{4.1}$$

and obtain $p_j = q_j\tau_j(q_j)$.

The coupling conditions at the junctions read

For junctions of merging type:

$q_k = q_i + q_j$

For junctions of dispersing type:

$q_i + q_j = q_k.$

For all roads

$M_j \geq q_j \geq 0.$

Note that the control variable α_v does not appear in the above formulation. Therefore the values of q_i, q_j are not solely defined by q_k. The functional J is given in terms of q_j by

$$J(q_1, \dots, q_{|E|}; T, \rho_0) = \sum_{j=1}^{|E|} \Big(TL_j - t_j L_j - \frac{\tau_j(q_j) L_j^2}{2} \Big) \tau(q_j) q_j. \tag{4.2}$$

Then the complete model and the optimization problem reads

$$\min_{q_j} J(q_1, \dots, q_{|E|}; T, \rho_0)$$

where for junctions of dispersing type:

$$t_i = t_j = t_k + L_k \tau_k(q_k)$$

$$q_i + q_j = q_k$$

where for junctions of merging type:

$$t_k = (t_i + L_i \tau_i(q_i)) \frac{q_i \tau_i(q_i)}{q_i \tau_i(q_i) + q_j \tau_j(q_j)} + (t_j + L_j \tau_j(q_j)) \frac{q_j \tau_j(q_j)}{q_i \tau_i(q_i) + q_j \tau_j(q_j)}$$

$$q_k = q_i + q_j$$

where for roads ingoing to the network:

$$q_j = f_0(\rho_0), t_j = 0$$

and where for all roads:

$$M_j \geq q_j \geq 0$$

We derive different (linear!) models from this formulation and refer to the subsequent sections for numerical results.

4.1 Linear models with dynamics

The coupling conditions at the junctions are linear for q_j but nonlinear for t_j. We use different possibilites to linearize the coupling t_j. In the numerical tests it turns out that the crucial point is the proper discretization of the weight w appearing in the case of merging junctions, i. e.,

$$w_i(q_i, q_j) := \frac{q_i \tau_i(q_i)}{q_i \tau_i(q_i) + q_j \tau_j(q_j)}, \qquad w_j(q_i, q_j) := \frac{q_j \tau_j(q_j)}{q_i \tau_i(q_i) + q_j \tau_j(q_j)}$$

We propose two different approaches and compare the results numerically in Section 5.

A We approximate

$$w_i, w_j \sim \tilde{w} = \frac{1}{2}$$

and calculate the first order Taylor expansion $\tilde{\tau}_j(q) = \tau_j(0) + q\tau_j'(0)$ as an approximation for $\tau_j(q)$. Neglecting higher order terms, we obtain the

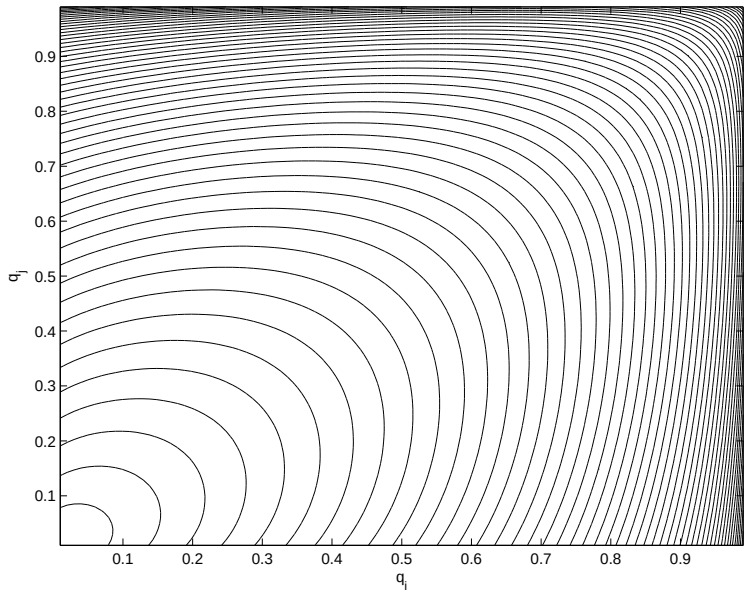

Figure 2: Contour lines of the nonlinear weight function $a_k(q_i, q_j)$ for $q_i, q_j \in [0, 1]$

following linear equations:

$$\begin{aligned} &\text{Dispersing junctions} \\ &t_i = t_j = t_k + L_k \tilde{\tau}_k(q_k) \\ &\text{Merging junctions} \\ &t_k = \big(t_i + L_i \tilde{\tau}_i(q_i)\big) \cdot \tilde{w} + \big(t_j + L_j \tilde{\tau}_j(q_j)\big) \cdot \tilde{w}. \end{aligned} \tag{4.3}$$

B The junctions of merging type are now approximated by piecewise linear functions on triangles, a more refined approximation as in case A. Let

$$a_k(q_i, q_j) := L_i \tau_i(q_i) \frac{q_i \tau_i(q_i)}{q_i \tau_i(q_i) + q_j \tau_j(q_j)} + L_j \tau_j(q_j) \frac{q_j \tau_j(q_j)}{q_i \tau_i(q_i) + q_j \tau_j(q_j)} \tag{4.4}$$

As an example note that for $f(\rho) = 4\rho(1 - \rho/M_i)$ and $M_i = M_j = 1$ the contour lines of a_k are given in Figure 2.

At each junction k of merging type, for a_k we introduce $N_i \cdot N_j$ discretization points (ξ_v^k, η_w^k) with $0 = \xi_1^k < \xi_2^k < \ldots < \xi_{N_i - 1}^k < \xi_{N_i}^k = M_i$ and $0 = \eta_1^k < \eta_2^k < \ldots < \eta_{N_j - 1}^k < \eta_{N_j}^k = M_j$. Denote Δ a partition of the grid of discretization points into triangles and introduce a binary variable $y_{(p_1,p_2,p_3)}^k \in \{0, 1\}$ for each triangle $(p_1, p_2, p_3) \in \Delta$. The identification of the proper triangle corresponding to the incoming fluxes q_i, q_j is done by the next equations. Exactly one triangle has to be selected:

$$\sum_{(p_1,p_2,p_3) \in \Delta} y_{(p_1,p_2,p_3)}^k = 1. \tag{4.5}$$

Once one triangle is selected, the values of q_i, q_j can be encoded as convex combination of its corners. For this, introduce a fractional variable $\lambda_{v,w}^k \geq$

0 for each discretization point (ξ_v^k, η_w^k), which are coupled to q_i and q_j as follows:

$$q_i = \sum_{v=1}^{N_i} \sum_{w=1}^{N_j} \xi_v^k \cdot \lambda_{v,w}, \qquad q_j = \sum_{v=1}^{N_i} \sum_{w=1}^{N_j} \eta_w^k \cdot \lambda_{v,w}. \tag{4.6}$$

The convex combination condition is

$$\sum_{v=1}^{N_i} \sum_{w=1}^{N_j} \lambda_{v,w} = 1. \tag{4.7}$$

Only those three values $\lambda_{p_1}, \lambda_{p_2}, \lambda_{p_3}$ are non-zero that are corresponding to the selected triangle by equation (4.5):

$$y^k_{(p_1,p_2,p_3)} \leq \lambda_{p_1} + \lambda_{p_2} + \lambda_{p_3}, \qquad \forall\ (p_1, p_2, p_3) \in \Delta. \tag{4.8}$$

To introduce $\tilde{a}_k$ as a piecewise linear approximation of $a_k(q_i, q_j)$, we add the following equation to the model:

$$\tilde{a}_k = \sum_{v=1}^{N_i} \sum_{w=1}^{N_j} a_k(\xi_v, \eta_w) \cdot \lambda_{v,w} \tag{4.9}$$

The junctions of dispersing type are approximated as in case A, whereas for the junctions of merging type, we use a blending of $\tilde{a}$ as above and $\tilde{w}$ as in case A:

$$\begin{aligned} &\text{Dispersing junctions} \\ &t_i = t_j = t_k + L_k \tilde{\tau}_k(q_k) \\ &\text{Merging junctions} \\ &t_k = (t_i + t_j) \cdot \tilde{w} + \tilde{a}_k. \end{aligned} \tag{4.10}$$

For any linearization A or B we linearize the functional (4.2) as follows. For every $j \in E$ we introduce D_q variables $0 \leq y_i^j \leq \frac{M_j}{D_q}$ and let the flux be represented by

$$q_j = \sum_{i=1}^{D_q} y_i^j. \tag{4.11}$$

Functional J is approximated by

$$\tilde{J}(q_1, \ldots, q_{|E|}; T, \rho_0) := \sum_{j=1}^{|E|} z_j, \tag{4.12}$$

where we introduce for every edge $j \in E$ and every $k = 1, \ldots, D_t$ the inequality

$$\begin{aligned} &\sum_{i=1}^{D_q} \left(G\left(\frac{(i+1) \cdot M_j}{D}, T \cdot 2^{k-D_t} \right) - G\left(\frac{i \cdot M_j}{D}, T \cdot 2^{k-D_t} \right) \right) \cdot \frac{D}{M_j} \cdot y_i^j \\ \leq\ & z_j + M \cdot (1 - u_{jk}), \end{aligned} \tag{4.13}$$

where M is a sufficient big value and G is defined by

$$G(\xi,\zeta) := \left(T - \zeta - \frac{\tau(\xi)L_j}{2}\right) \cdot L_j\tau(\xi)\xi, \tag{4.14}$$

and we assume that $G(\cdot,\zeta)$ is convex for every $\zeta \in [0,T]$. Moreover, u_{jk} is a binary variable for every $j \in E$ and $k = 1,\dots,D_t$, where $u_{jk} = 1$ if $t_j \leq T \cdot 2^{k-D_t}$. Thus we add the following inequalities to the model:

$$t_j \geq T \cdot 2^{k-D_t}(1 - u_{jk}), \tag{4.15}$$

for all $j \in E$ and $k = 1,\dots,D_t$. Summarizing we obtain a linear mixed-integer model with dynamics given by

$$\min_{q_j} \tilde{J}(q_1,\dots,q_{|E|};T,\rho_0)$$
where for junctions of dispersing type:
$t_i = t_j = t_k + L_k\tilde{\tau}_k(q_k)$
$q_i + q_j = q_k$
where for junctions of merging type:
case A: $t_k = \left(t_i + L_i\tilde{\tau}_i(q_i)\right) \cdot \tilde{w} + \left(t_j + L_j\tilde{\tau}_j(q_j)\right) \cdot \tilde{w}$
case B: $t_k = (t_i + t_j) \cdot \tilde{w} + \tilde{a}_k$
$q_k = q_i + q_j$
where for roads ingoing to the network:
$q_j = f_0(\rho_0), t_j = 0$
and where for all roads:
$M_j \geq q_j \geq 0.$

Remark 4.1. *In the above modelling we set the discretization points as $T2^{k-D_t}$ for $k = 1,\dots,D_t$. This produces a log-scale distribution of discretization points in $[0,T]$. Other distributions are also possible. For example, if we equally distribute we obtain*

$$t_j \geq T\frac{k-1}{D_t - 1}(1 - u_{jk}) \tag{4.16}$$

instead of equation (4.15). The proper choice depends on the size of the network geometry and the scaling of T.

4.2 Linear model without dynamics

We assume $t_j = 0$ which models a static traffic flow network. We obtain a linear functional $\tilde{J}$ from (4.2) by a piecewise linear approximation of J. For this, we introduce D variables $0 \leq y_i^j \leq \frac{M_j}{D}$ for every edge $j \in E$. Then the flux q_j is represented by

$$q_j = \sum_{i=1}^{D} y_i^j. \tag{4.17}$$

Now J is approximated by

$$\tilde{J}(q_1,\dots,q_{|E|};T,\rho_0) := \sum_{j=1}^{|E|}\sum_{i=1}^{D}\left(G\left(\frac{(i+1)\cdot M_j}{D}\right) - G\left(\frac{i\cdot M_j}{D}\right)\right)\cdot\frac{D}{M_j}\cdot y_i^j, \tag{4.18}$$

where G is defined by

$$G(\xi) := \left(TL_j - \frac{\tau(\xi)L_j^2}{2}\right)\cdot\tau(\xi)\cdot\xi. \tag{4.19}$$

Again, we assume $G(\cdot)$ to be convex. Summarizing, we have the following model

$$\min_{q_j} \tilde{J}(q_1,\dots,q_{|E|};T,\rho_0)$$

where for roads connected to a junction v:

$$\sum_{j\in\delta_v^+} q_j = \sum_{j\in\delta_v^-} q_j$$

where for roads ingoing to the network:

$$q_j = f_0(\rho_0)$$

and where for all roads:

$$M_j \geq q_j \geq 0.$$

4.3 Linearization for monotone, non-convex function G

In both linearizations above we assumed $G(\cdot,\zeta)$ and $G(\cdot)$, respectively, to be convex functions. The convexity depends on τ and is satisfied for those functions τ we study within this article. However, other choices for τ are possible, where G is non-convex. But, if G happens to be monotone (and non-convex), it is still possible to obtain a linearization. We present the necessary changes to the model only in the case without dynamics. In the dynamic case they are similar.

We introduce D variables $y_i^j \geq 0$ for every edge $j \in E$. Since G is non-convex, they cannot be coupled to the flux q_j as simple as in (4.17). Instead we have to use the following inequalities

$$q_j \leq y_i^j + \frac{M_j}{D}\cdot i, \qquad \forall\, i = \{1,\dots,D\}, j \in A. \tag{4.20}$$

Now J is approximated by

$$\tilde{J}(q_1,\dots,q_{|E|};T,\rho_0) := \sum_{j=1}^{|E|}\frac{D}{M_j}\Big(G\left(\frac{M_j}{D}\right)\cdot y_0^j + \tag{4.21}$$

$$\sum_{i=2}^{D}\left(G\left(\frac{(i+1)\cdot M_j}{D}\right) - 2\cdot G\left(\frac{i\cdot M_j}{D}\right) + G\left(\frac{(i-1)\cdot M_j}{D}\right)\right)\cdot\frac{D}{M_j}\cdot y_i^j\Big),$$

where G is defined as before.

4.4 Mincost flow type model

We again assume $t_j = 0$, i.e. the static network case. Instead of a piecewise linear approximation of our functional (4.2) we additionally assume a simplified dynamic: If the function

$$u_j^e(\rho) = c_j = \text{ const}_j$$

is constant for all j, then by definition

$$\tau(q_j) = \frac{1}{c_j}.$$

The functional (4.2) reads

$$\bar{J}(q_1, \ldots, q_{|E|}; T, \rho_0) = \sum_{j=1}^{|E|} \omega_j q_j \tag{4.22}$$

where ω_j are constants given by

$$\omega_j = T\frac{L_j}{c_j} - \frac{L_j^2}{2c_j^2}.$$

Together with the linear coupling conditions and the lower bounds for q_j we obtain the classical min-cost flow problem:

$$\min_{q_j} \sum_{j=1}^{|E|} \omega_j q_j$$

where for roads connected to a junction v:

$$\sum_{j \in \delta_v^+} q_j = \sum_{j \in \delta_v^-} q_j$$

where for roads ingoing to the network:

$$q_j = f_0(\rho_0)$$

and where for all roads:

$$M_j \geq q_j \geq 0$$

Remark 4.2. *Unfortunately the assumption $u_j^e = \text{constant}_j$ is not a realistic approximation of a typical fundamental diagram. For reasonable fundamental diagrams we refer to [22]. At least we have to assume $u_j^e(x)$ is linear.*

We have the following remark on the relation of the linear models given above and known other approaches.

Remark 4.3. *In [25] also linear models are introduced. There the starting point are the "transit times" τ_e which are assumed to be known functions. They describe the time needed by a flow to pass the arc e. In our formulation the "transit times" are the functions derived by equation (4.1), i. e.,*

$$q \to \tau_j(q) L_j.$$

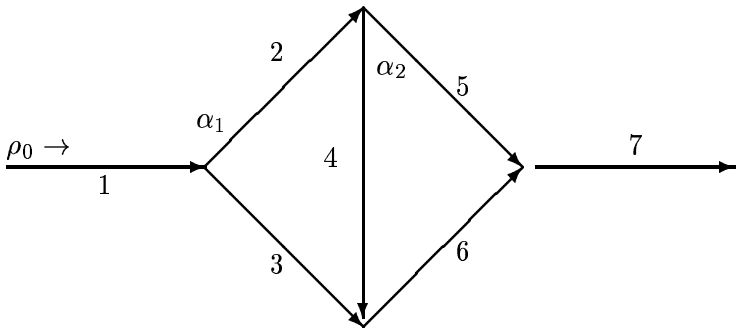

Figure 3: Example of a network

The case of constant transit times is named "static flow problems" in [25]. In our introduced model this reflects the situation $u_j^e(\rho)$ constant. As pointed out by Möhring, et. al. this can not be a realistic assumption. Therefore, they introduced "static traffic flows with congestion" by assuming a dependency of τ_e on q. In our model this approach is reflected by the introduced linear model without dynamics. However, we see by our derivation that congestion in form of backwards going shock waves are not covered by those models, c.f. numerical results below.

5 Results

We compared the computing times for different models and networks. All results have been obtained on a 1.0Ghz Pentium III processor machine with 2 GB RAM, 256 KB first level cache and Debian Linux v3.0 as operating system.

5.1 Testcase for comparing network models

For the purpose of comparing the models we introduce a network with two controls and seven roads as in Figure 3. As an example we use the smooth and concave family of flux functions

$$f_j(\rho) = \rho u_j^e(\rho) = 4\rho(1 - \rho/M_j). \tag{5.1}$$

The function $\tau_j(\rho)$ is then given by (4.1), i. e.,

$$\tau_j(q) = \frac{M_j}{2\left(M_j + \sqrt{M_j^2 - M_j q}\right)}, \quad 0 \le q \le M_j. \tag{5.2}$$

If not stated otherwise we assume

$$T = 5 \text{ and } L_j := b_j - a_j = 1 \ \ \forall j = 1, \ldots, 7. \tag{5.3}$$

We define q_0 to be the known inflow given at $x = a_1$.

5.1.1 Comparison of the functional values

We compare the derived models on the sample network. We compute the functional of the corresponding model for all admissible choices of the control variables α_1 and α_2. In the context of the linear models this implies to compute the objective for all choices $q_1, \dots, q_7$ satisfying the constraints. As described in Section 4 the fluxes q_j and the controls are related. For example we obtain for the first roads of our sample network

$$q_1 = q_0,\ q_2 = \alpha_1 q_1,\ q_3 = (1-\alpha_1)q_1.$$

In all subsequent plots we draw contour lines of the functional against α_1 and α_2. We choose different maximal fluxes M_j on the roads to obtain different test-cases.

Testcase 1: Free Flow

We set $M_j = 1$ for all roads and $q_0 = 96\% M_1$. We compute the functional (2.15) by a trapezoid rule. The underlying partial differential equations is solved by a first-order Godnuov scheme with $N = 100$ discretization points for each road j. The functional (3.5) is computed by the formulas given in Section 3. For the linear models we computed the functional (4.21) with $D = 1000$ variables for each edge j. Note, that the function $\xi \to G(\xi)$ is at least monotone for the choice (5.1). For comparison we include a plot of the functional for the mincostflow problem (4.22) where we set $u_j^e(\rho) = 2$ for this calculation. The results are given in Figure 4. The minimizer of all problems is $(\alpha_1, \alpha_2) = (\frac{1}{2}, 0)$. In case of the mincostflow model we loose the uniqueness of the minimizer. Furthermore, the qualitative behaviour differs significantly from the other models.

Testcase 2: Backwards going shock waves

When deriving the simplified models we neglected backwards going shock waves. This was an essential part of the simplification of the dynamics. We compare the simplified nonlinear model with the model based on partial differential equations in a case with backwards going shock waves. We set $M_1 = M_2 = M_4 = M_6 = 2,\ M_3 = 1,\ M_5 = 0.5$ and $q_0 = 75\% M_1$. We used the same discretization as previoulsy and compare the contour lines of (2.15) and (3.5) in Figure 5). We observe that the domain of admissible controls is larger in the pde case due to the occurence of backwards going waves. The region for the optimal control coincides. We skip results on the linear model since they approximate the algebraic model.

Testcase 3: Neglecting dynamics

For the linear and simplified nonlinear models we considered models with and without dynamics. In this testcase we highlight the effects appearing when neglecting the dynamics. We compute the corresponding functionals (4.21) and (4.12) for the following setting $M_j = 2,\ q_0 = 96\% M_1$ and $L_1 = L_7 = L_5 = 2, L_4 = L_6 = 1, L_2 = 2.5, L_3 = 15$. In the dynamic case we allow only those controls α_1, α_2 where the incoming flux reaches $x = b_7$, i. e., $t_7 \leq T$. The

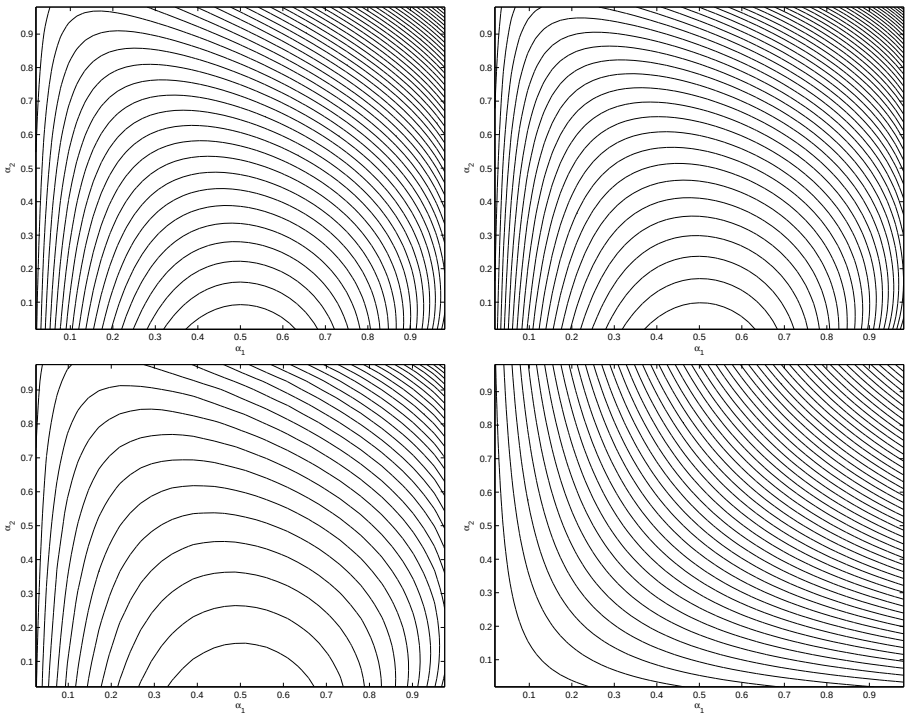

Figure 4: Testcase 1: Contour lines of the functionals for partial differential equation, simplified nonlinear, linear without dynamics and mincostflow model (top left to bottom right).

simplified nonlinear model with dynamics is given in Section 3. For the model without dynamics we set

$$t_j = 0 \quad \forall j = 1, \ldots, 7.$$

The results are in Figure 6. Note, that in the region $\alpha_1 < 30\%$ the routed traffic does not reach the outgoing road. Furthmore, the functionals differ significantly in their qualitative behaviour.

Testcase 4: Discretization points for linear models

The linear models depend strongly on the number of discretization points D. We study the qualitative behaviour of the contour lines when decreasing D. We consider the linear model without dynamics and its functional (4.21). We set $M_j = 1, q_0 = 0.96\%$. We plot the contour lines for $D = 5$ and $D = 25$ discretization points in Figure 7.

Testcase 5: Linearization of the dynamics

In this case we consider the influence of the various possible discretizations for the coupling in t_j. We consider the same setting as in Testcase 3. We compare the qualtiative behaviour of the functional for the simplified nonlinear model with the linear models with dynamics given in Section 4.1. We compare the different discretization, Cases A and B. The results are given in Figure 8. We used $D_q = D_t = 100$ variables for the discretization of the flux and the time

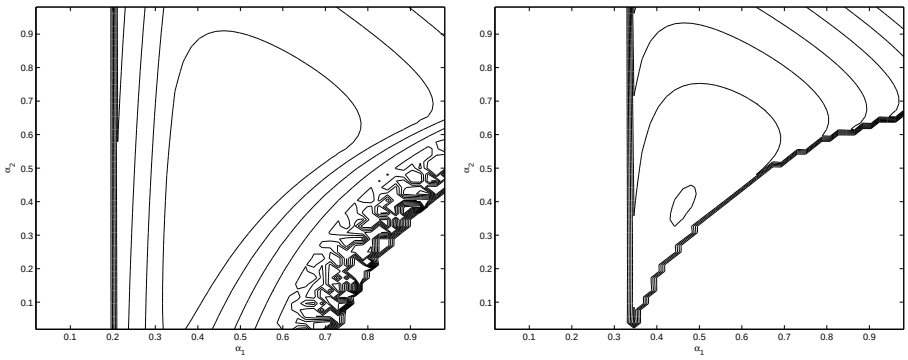

Figure 5: Testcase 2: Contour lines for the functionals for pde and simplified nonlinear model (left to right).

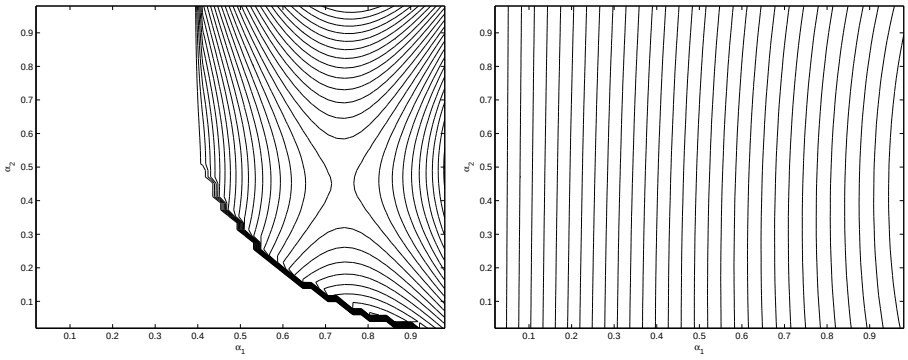

Figure 6: Testcase 3: Contour lines for the functionals for simplified model with (left) and without dynamics.

on each road for any linearized model. We calculate Cases B with $N_i = N_j = 5$ and $N_i = N_j = 25$, respectively, discretization points for each junction of the merging type.

5.1.2 Optimization on the sample network

We consider the optimization problems introduced and compare computing times on the sample network.

As in the previous section we solved the partial differential equations model with a Godunov scheme with N discretization points. The functional is discretized using the trapezoid rule. For standard nonlinear optimization routines we need at least the gradient of the functional. We compute an approximation by finite differences. Other approaches (using adjoint formulas) are investigated in [15]. In case of the algebraic model the gradient can be calculated analytically.

For all nonlinear optimization problems the L-BFGS-B optimizer of Byrd, Lu, Nocedal and Zhu [4, 33, 5] is used. This method is a gradient projection

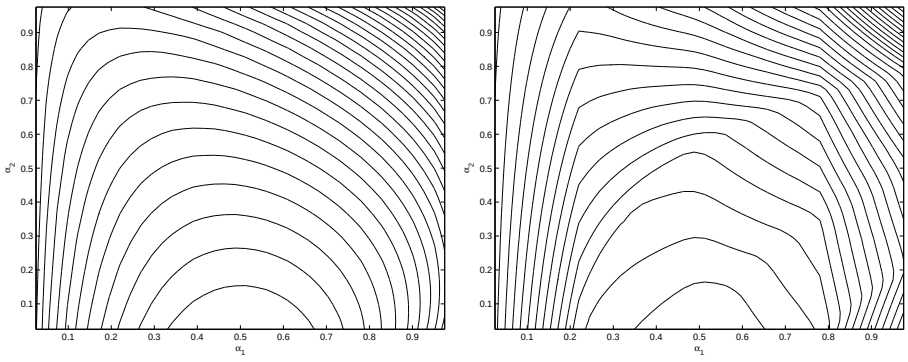

Figure 7: Testcase 4: Contour lines for the functionals for linear model without dynamics and varying $D = 25$ (left), resp. $D = 5$ (right).

method with a limited memory BFGS approximation of the Hessian and is capable to consider bound constraints. The default settings are $m = 17, factr = 1.d + 5, pgtol = 1.d - 8$ and $isbmin = 1$.

The linear model without dynamic is a pure linear programming problem. We solved it using ILOG CPLEX 8.1 [20]. As a default strategy, we set the network simplex method to solve the linear programs. For our test-cases, this method outperforms other solution techniques, such as primal or dual simplex. In case of the linear model with dynamics we have a mixed-integer problem. We consider the discretization (a) of the dynamics only. Among the currently most successful methods for solving these problems are linear programming based branch-and-bound algorithms, where the underlying linear programming relaxations are possibly strengthend by cutting planes. Fortunately, todays state-of-the-art commercial MIP-solvers (such as CPLEX [20]) are able to handle mixed-integer programs even for our large size problem instances.

For the setting of Testcase 1 we have the following result on the computational times (CPU times), see Figure 9. The parameters (D_q, D_t) describes the discretization of the nonlinear functional. The parameter $N_i N_j$ describes the number of discretization points for the function $a_k(\cdot, \cdot)$ at the merging junctions. Therefore, the only models reasonable to test on large scale networks are the simplified nonlinear and the linear models.

5.2 Large Scale Network Optimization

The network considered next is shown in Figure 10.

There, every node in the top row is controlable via a separate control α_v. There are only one source and one sink. The prescribed inflow is again $q_0 = 96\% M_1$ and all streets have the same maximal flux, $M_j = 1.0$ Then, the optimal controls are $\alpha_1 = 0.5$ and $\alpha_v = 1.0$, $\forall v \neq 1$. The results are given in Figure 11. The number of discretization points for the flux q per road is denoted by D_q and for the time by D_t. The number of discretization points

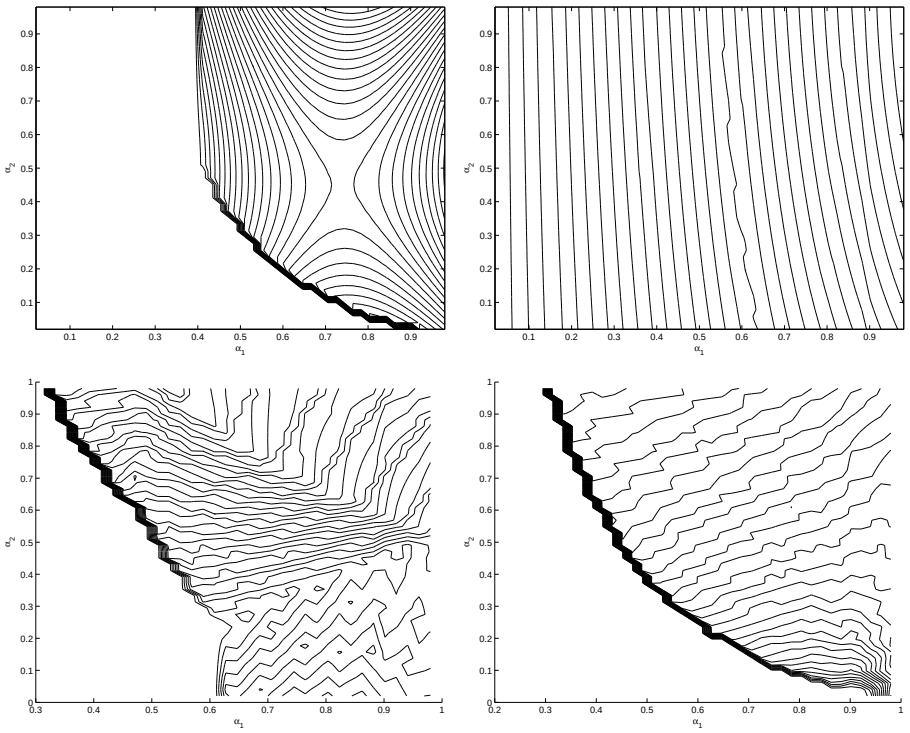

Figure 8: Testcase 5: Contour lines for the functionals for simplified nonlinear and different linear models with dynamics. Simplified nonlinear (upper left), Case A (upper right), Case B with $N_i = N_j = 5$, resp. $N_i = N_j = 25$ (lower row left to right)

for each function a_k, c.f. equation (4.4), in model B is denoted by $N_i N_j$. Note that all nodes in the bottom row are of the merging type. To improve the performance of CPLEX we increased the optimiality gap from 1/1000 (default setting) to 10%. We present results for other optimality gaps, too.

6 Summary

- A hierachy a traffic network models ranging from PDE models to simple combinatorial models of mean-cost-flow type has been developed. The introduced linear models without dynamics are similar to the models de-

Model and Scheme	Parameters	CPU time
Godunov scheme for pde model	N=100	135.65 s
Godunov scheme for pde model	N=50	45.17 s
Simplified nonlinear model		0.05 s
Linear Model with dynamics (A,B)	$D_q = D_t = 100, N_i N_j = 25$	0.02 s
Linear Model without dynamics	$D_q = 100$	0.01 s

Figure 9: CPU times for sample network and different models

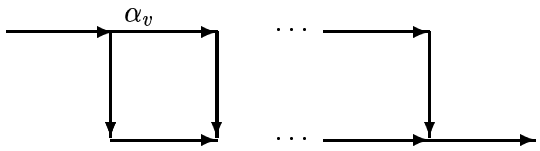

Figure 10: General layout of a large scale network

veloped in [25].

- However, the simplified models developed here do not contain dynamic situations with backwards going shocks, i.e., traffic jams. To include such situations more complicated models have to be derived from the underlying PDE network.
- A variety of different network topologies has been investigated. Combinatorial and continuous optimization approaches using these models have been implemented and compared.

Acknowledgements

The presented work has been partially supported by Deutsche Forschungsgemeinschaft (DFG), KL 1105/5. We also thank Rolf Möhring for his valuable comments on time dependent network flow models.

References

[1] A. Aw and M. Rascle, *Resurrection of second order models of traffic flow*, SIAM J. Appl. Math., 60 (2000), pp. 916–938.

[2] C. Bardos, A. LeRoux, and J. Nedelec, *First order quasilinear equations with boundary conditions*, Comm. in partial differential equations, 4 (1979), pp. 1017–1034.

[3] M. Blinkin, *Problem of optimal control of traffic flow on highways*, Automation and Remote Control, 37 (1976), pp. 662–667.

[4] R. Byrd, P. Lu, J. Nocedal, and C. Zhu, *A limited memory algorithm for bound constrained optimization*, SIAM J. Sci. Comp., 16 (1995), pp. 1190–1208.

[5] R. Byrd, J. Nocedal, and R. Schnabel, *Representations of quasi-newton matrices and their use in limited memory methods*, Mathematical Programming, 63 (1994), pp. 129–156.

Model	# Roads	D_q	D_t	N_iN_j	Gap	CPU time
Simplified nonlinear model	240	n.a.	n.a.	n.a.	n.a.	6 s
Linear with dynamics (B)		10	10	25	1%	11 m
		10	10	25	10%	3.8 m
		10	10	9	0.1%	2.6 m
		10	10	9	10%	57 s
Linear with dynamics (A)		100	10	n.a.	0.1%	33.08 s
		10	10	n.a.	0.1%	4.78 s
Linear without dynamics		100	n.a.	n.a.	0.1%	<0.01 s
Simplified nonlinear model	1'500	n.a.	n.a.	n.a.	n.a.	57 m
Linear with dynamics (B)		10	10	25	10%	4.7 h
		10	10	9	10%	26 m
		5	5	9	10%	5 m
Linear with dynamics (A)		100	10	n.a.	0.1%	180.01 m
		10	10	n.a.	0.1%	13.69 m
Linear without dynamics		1000	n.a.	n.a.	0.1%	24.98 s
		100	n.a.	n.a.	0.1%	12.75 s
		5	n.a.	n.a.	0.1%	1.8 s
Simplified nonlinear model	15'000	n.a.	n.a.	n.a.	n.a.	>4d
Linear with dynamics (B)		5	5	9	10%	6.2 h
Linear without dynamics		100	n.a.	n.a.	n.a.	22.79 m
		10	n.a.	n.a.	n.a.	7.33 m
Linear without dynamics	150'000	10	n.a.	n.a.	n.a.	16.77 h

Figure 11: CPU times for large scale networks. n.a. is short for not available since those quantities do not appear in the corresponding models.

[6] M. Carey and E. Subrahmanian, *An approach for modeling time-varying flows on congested networks*, Transp. Res. B, (2000), pp. 157–183.

[7] G. Coclite and B. Piccoli, *Traffic flow on a road network*, to appear in SIAM J. Math. Anal.

[8] R. Colombo, *Hyperbolic phase transitions in traffic flow*, SIAM J. on Appl. Math., 63 (2002), pp. 708–721.

[9] C. M. Dafermos, *Polygonal approximations of solutions of the initial value problem for a conservation law*, J. Math.Anal.Appl., 38 (1972), pp. 33–41.

[10] L. Ford and D. Fulkerson, *Constructing maximal dynamic flows from static flows*, Operations Research, (1958), pp. 419 – 433.

[11] J. Greenberg, *Extension and amplification of the Aw-Rascle model*, SIAM J. Appl. Math., 62 (2001), pp. 729–745.

[12] J. Greenberg, A. Klar, and M. Rascle, *Congestion on multilane highways*, SIAM J. Appl. Math., 63 (2003), pp. 818–833.

[13] M. Günther, A. Klar, T. Materne, and R. Wegener, *Multivalued fundamental diagrams and stop and go waves for continuum traffic flow equations*, to appear in SIAM J. Appl. Math.

[14] D. Helbing, *Improved fluid dynamic model for vehicular traffic*, Physical Review E, 51 (1995), p. 3164.

[15] M. Herty, M. Gugat, A. Klar, and G. Leugering, *Optimal control for traffic flow networks*, preprint, (2003).

[16] M. Herty and A. Klar, *Modelling, simulation and optimization of traffic flow networks*, SIAM J. Sci. Comp., 25 (2003), pp. 1066–1087.

[17] ——, *Simplified dynamics and optimization of large scale traffic networks*, M3AS, 14 (2004), pp. 1–23.

[18] H. Holden and N. Risebro, *A mathematical model of traffic flow on a network of unidirectional road*, SIAM J.Math.Anal., 4 (1995), pp. 999–1017.

[19] ——, *Front tracking for hyperbolic conservation laws*, Springer, New York, Berlin, Heidelberg, 2002.

[20] ILOG CPLEX Division, *Using the CPLEX Callable Library*, 889 Alder Avenue, Suite 200, Incline Village, NV 89451, USA, 2000. Information available at URL http://www.cplex.com.

[21] O. Jahn, R. Möhring, and A. S. Schulz., *Optimal routing of traffic flows with length restrictions in networks with congestion*, in Operations Research Proceedings, K. I. et al., ed., Berlin, 2000, Springer-Verlag, pp. 437 – 442.

[22] A. Klar, R. Kuehne, and R. Wegener, *Mathematical models for vehicular traffic*, Surv. Math. Ind., 6 (1996), p. 215.

[23] A. Klar and R. Wegener, *Kinetic derivation of macroscopic anticipation models for vehicular traffic*, SIAM J. Appl. Math., 60 (2000), pp. 1749–1766.

[24] E. Köhler and M. Skutella, *Flows over time with load-dependent transit times*, in Proceedings of the 13th Annual ACM-SIAM Symposium on Discrete Algorithms, 2002, pp. 174 – 183.

[25] E. Köhler, M. Skutella, and R. H. Möhring, *Traffic networks and flows over time*, preprint no. 752/2002, (2002).

[26] A. Kotsialos, M. Papageorgiou, M. Mangeas, and H. Haj-Salem, *Coordinated and integrated control of motorway networks via non-linear optimal control*, Transport Research Part C, 10 (2002), pp. 65–84.

[27] R. Kühne, *Macroscopic freeway model for dense traffic*, in 9th Int. Symp. on Transportation and Traffic Theory,VNU Science Press, Utrecht, N. Vollmuller, ed., 1984, pp. 21–42.

[28] K. Langkau, *Flows Over Time with Flow-Dependent Transit Times*, PhD thesis, Fakultät II, Institut für Mathematik, Technische Universität Berlin, 2003.

[29] M. Lighthill and J. Whitham, *On kinematic waves*, Proc. Royal Soc. Edinburgh, A229 (1983), pp. 281–345.

[30] P. Nelson, *A kinetic model of vehicular traffic and its associated bimodal equilibrium solutions*, Transport Theory and Statistical Physics, 24 (1995), pp. 383–408.

[31] H. Payne, *FREFLO: A macroscopic simulation model of freeway traffic*, Transportation Research Record, 722 (1979), pp. 68–75.

[32] G. Whitham, *Linear and Nonlinear Waves*, Wiley, New York, 1974.

[33] C. Zhu, R. Byrd, J. Lu, and J. Nocedal, *L-bfgs-b: Fortran subroutines for large scale bound constrained optimization*, Tech. Report, NAM-11, EECS Department, Northwestern University, (1994).